Variability of glenohumeral positioning and bone-to-tendon marker length measurements in repaired rotator cuffs from longitudinal computed tomographic imaging

Bong-Jae Jun, PhD [a], Sambit Sahoo, MD, PhD [a], Peter B. Imrey, PhD [b], Andrew R. Baker, MS [a], Ahmet Erdemir, PhD [a], Yuxuan Jin, MS [b], Joseph P. Iannotti, MD, PhD [c], Vahid Entezari, MD, MMSc [c], Eric T. Ricchetti, MD [c], Michael J. Bey, PhD [d], Kathleen A. Derwin, PhD [a,*]

[a] Department of Biomedical Engineering, Cleveland Clinic, Cleveland, OH, USA
[b] Department of Quantitative Health Sciences, Cleveland Clinic, Cleveland, OH, USA
[c] Department of Orthopaedic Surgery, Cleveland Clinic, Cleveland, OH, USA
[d] Department of Orthopaedic Surgery, Bone and Joint Center, Henry Ford Hospital, Detroit, MI, USA

ARTICLE INFO

Background: To address the need for more objective and quantitative measures of tendon healing in research studies, we intend to use computed tomography (CT) with implanted radiopaque markers on the repaired tendon to measure tendon retraction following rotator cuff repair. In our small prior study, retraction at 1-year follow-up averaged 16.1± 5.3 mm and exceeded 10.0 mm in 12 of 13 patients, and thus tendon retraction appears to be a common clinical phenomenon. This study's objectives were to assess, using 5 longitudinal CT scans obtained over 1 year following rotator cuff repair, the variability in glenohumeral positioning because of pragmatic variations in achieving perfect arm repositioning and to estimate the associated measurement variability in bone-to-tendon marker length measurements.
Methods: Forty-eight patients underwent rotator cuff repair with intraoperative placement of radiopaque tendon markers at the repair site. All patients had a CT scan with their arms at the side on the day of surgery and at 3, 12, 26, and 52 weeks postoperatively. Glenohumeral position (defined by the orientation and distance of the humerus with respect to the scapula) and bone-to-tendon marker lengths were measured from each scan. Within-patient variation in glenohumeral position measurements was described by their pooled within-patient standard deviations (SDs), and variation in bone-to-tendon marker lengths by their standard errors of measurement (SEMs) and 95% confidence level minimally detectable distances (MDD_{95}) and changes (MDC_{95}).
Results: The mean glenohumeral orientation from the 5 longitudinal CT scans averaged across the 48 patients was 12.6° abduction, 0.4° flexion, and −0.1° internal rotation. Within-patient SDs (95% confidence intervals) of glenohumeral orientation were 3.0° (2.7°-3.4°) in extension/flexion, 5.2° (4.6°-5.8°) in abduction/adduction, and 8.2° (7.3°-9.2°) in internal/external rotation. The SDs of glenohumeral distances were less than 1 mm in any direction. The estimated SEMs of bone-to-tendon lengths were consistent with a common value of 2.4 mm for any of the tendon markers placed across the repair, with MDD_{95} of 4.7 mm and MDC_{95} of 6.7 mm.
Conclusion: Apparent tendon retraction of 5 mm or more, when measured as the distance from a tendon marker's day of surgery location to its new location on a volumetrically registered longitudinal CT scan, may be considered above the usual range of measurement variation. Tendon retraction measured using implanted radiopaque tendon markers offers an objective and sufficiently reliable means for quantifying the commonly expected changes in structural healing following rotator cuff repair.

---

* Corresponding author: Kathleen A. Derwin, PhD, Department of Biomedical Engineering, ND-20, Lerner Research Institute, Cleveland Clinic 9500 Euclid Avenue, Cleveland, OH 44195, USA.
E-mail address: derwink@ccf.org (K.A. Derwin).

Healing following rotator cuff repair remains a significant clinical challenge. Recurrent tears have been reported for 10%-90% of the rotator cuff repairs,[5,15,20,30,33] depending on the patient's age and tear size.[22,25] Meta-analyses of the available literature has shown that the correlation between recurrent tears and clinical outcomes in the early to intermediate postoperative period ($\leq$5 years) following rotator cuff repair is weak on average and therefore of uncertain clinical importance.[8,24,27] The relationship is also inconsistent, as reports show that individually some patients with recurrent tears still have less pain and higher functional scores after surgery,[16,29,32] whereas patients with a structurally intact repair may demonstrate persistent degenerative muscle changes and shoulder weakness.[4,6,7,16] The weak and at times inconsistent correlation between recurrent tears and clinical outcomes following rotator cuff repair suggests a need for a deeper and more nuanced understanding of structural tendon healing.

Magnetic resonance imaging (MRI),[11,15,29] magnetic resonance arthrography,[1,10] and ultrasonography[14,21,23] are routinely used for diagnosing rotator cuff tears and repair integrity after surgery. Excellent sensitivity and specificity have been reported for each technique in terms of its binary diagnostic reliability.[13] A more granular classification of rotator cuff repair integrity using the 5-point Sugaya score can be used,[28] with fair to moderate exact inter-rater agreement (simple κ= 0.31-0.49)[9,19] and improved agreement when adjacent-category disagreements are penalized only minimally (weighted κ= 0.72).[14] Although these modalities constitute the current standard-of-care for diagnostic imaging of the rotator cuff, none can discern the type or quality of tissue at the repair site, and thus each faces challenges of clinical interpretation. To address the need for more objective and precise measures of tendon healing, we and others have developed a means by which to measure tendon retraction following rotator cuff repair using implanted radiopaque markers on the repaired tendon and 3-dimensional (3D) radiographic imaging.[2,18]

We broadly defined tendon retraction as the translation of the repaired tendon away from its position of initial fixation on the bone with or without formation of a recurrent defect. In a study involving 13 patients with rotator cuff repair, rotator cuff tendon retraction at 1-year follow-up after repair averaged 16.1 ± 5.3 mm (range 6-23 mm) and exceeded 10.0 mm in 12 of 13 patients.[18] Thus, tendon retraction appears to be a common clinical phenomenon, yet only 30% (4 of 13) of repairs were classified as structurally failed by MRI. This contrast between the continuous and categorical results suggests that "failure with continuity"—tendon retraction without the formation of a recurrent defect—might partially explain how patients with apparently structurally intact repairs on MRI might experience undesirable clinical outcomes.[4,6,7,16]

In another study of accuracy and repeatability of tendon retraction measurements in 6 patients with rotator cuff repair,[3] we observed that variation in repositioning the arm for repeat scanning could introduce variation in tendon retraction length measurements. The root mean square difference between bone-to-tendon length measurements on computed tomographic (CT) scans repeated twice on the same day, in arm positions such as the hand on umbilicus or hand at the side, was 1.3 mm.[3] Because tendon retraction in the clinical setting will derive from lengths measured on CT scans repeated longitudinally, we expect that pragmatic variation in glenohumeral position across longitudinal scans would also introduce variability into tendon retraction measures. Therefore, the objectives of this study were to (1) quantify the variability in glenohumeral positioning among 5 longitudinal CT scans obtained with the arm at the side in the first year

following rotator cuff repair and (2) estimate the associated measurement variability in bone-to-tendon marker length measurements due to pragmatic variations in achieving perfect arm repositioning across the scans.

Materials and methods

Patient longitudinal CT scanning

In this study, 48 patients participating in an ongoing, IRB-approved study (IRB 16-089, https://clinicaltrials.gov/ct2/show/NCT02716441) at our institution were analyzed. These patients had undergone arthroscopic repair of a rotator cuff tear involving the supraspinatus tendon with or without extension into the infraspinatus tendon. Following rotator cuff repair, radiopaque markers—either 1-mm tantalum beads (Halifax Biomedical, Mabou, Nova Scotia, Canada) in 18 patients or FibermarX tissue markers (Viscus Biologics LLC, Cleveland, OH, USA) in 30 patients—were tied to the superficial surface of the tendon. Tantalum beads were predrilled, threaded onto 5-0 Prolene and tied to a 2-0 Ti-Cron suture that was subsequently tied to the tendon surface. Markers were placed medial to the repair sutures at approximately 1-cm intervals in the anterior-posterior direction using a standard suture lasso and arthroscopic knot-tying technique. Given the variability in tear size, shape, and location across the cohort, between 2 and 5 radiopaque tendon markers were used per patient. Each tendon marker was named based on its anatomic location relative to the repair sutures and myotendinous junction. Specifically, T1, T3, T5, and T7 were used to name tendon markers just medial to the repair sutures, based on the involvement of the supraspinatus (T1, T3) and/or infraspinatus tendons (T5, T7). Similarly, T2, T4, and T6 were used to name markers placed on the repaired tendon more medially, near the myotendinous junction. The locations and appropriate labeling of the tendon markers were defined by visual inspection intraoperatively and subsequently confirmed against the bony anatomy on the day of surgery CT (CT$_{DOS}$) for each patient.

All the patients underwent 5 longitudinal CT scans: the CT$_{DOS}$ and at 3 (CT$_{WK003}$), 12 (CT$_{WK012}$), 26 (CT$_{WK026}$), and 52 weeks (CT$_{WK052}$) postoperatively. A low-dose scan protocol was performed (100-120 kVp, 45-60 mAs) on Siemens Definition Edge, Siemens Somatom Sensation 64 (0.6-mm slices; Siemens Medical Solutions, Malvern, PA, USA), GE Revolution EVO 64 (0.625-mm slices; GE Healthcare, General Electric Company, Boston, MA, USA), or Philips Brilliance 16 (0.8-mm slices; Philips Electronics N.A., Andover, MA, USA) scanners.[3,18,26] At the time of each CT scan, patients were instructed to lie supine and position the operated arm at the side, with hand on the thigh and thumb facing upward for consistency in arm positions across the longitudinal CT scans. The field of view was adjusted to enclose the shoulder joint, including the clavicle, scapula, and entire humerus. The entire image volume was reconstructed using a soft tissue kernel for image processing and analysis. Image processing was performed using custom software (RotatorCuffEvaluation, version 2.1.1; Cleveland Clinic, OH, USA) to load, segment, visualize, and register longitudinal CT images, identify the bony landmarks to define anatomic coordinate systems, and compute the 3D coordinates of the radiopaque markers with respect to the anatomic coordinate systems. The specific operations are described below.

CT image analysis

Scapular and humeral coordinate systems were defined from the reconstructed CT$_{DOS}$ images using bony landmarks (Fig. 1).
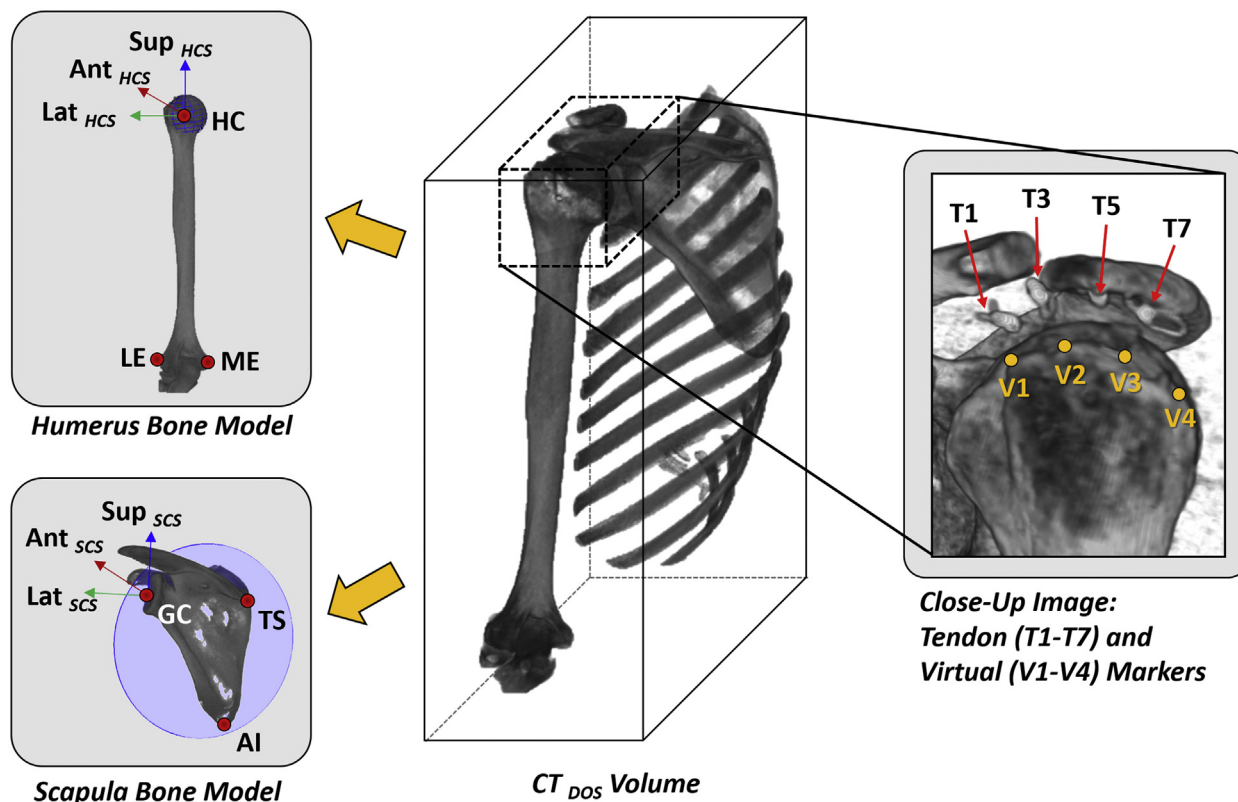
Figure 1 Representative shoulder computed tomography (CT) scan depicting the scapular and humeral bone models, respective bony landmarks and anatomic coordinate systems, virtual humeral markers (V1-V4), and tendon markers (T1, T3, T5, T7). *DOS*, day of surgery; *HC*, humeral head center; *LE*, lateral epicondyle; *ME*, medial epicondyle; *GC*, glenoid center; *TS*, trigonum scapulae; *AI*, angulus inferior; *Ant*, anterior; *Lat*, lateral; *Sup*, superior; *HCS*, humeral coordinate system; *SCS*, scapular coordinate system.

Similar to the International Society of Biomechanics guidelines for describing glenohumeral joint motion,[35] the scapular coordinate system was defined by the 3 bony landmarks of the glenoid center, trigonum scapulae, and angulus inferior. The humeral coordinate system was defined by the 3 bony landmarks of the humeral head center and the medial and lateral epicondyle. Any tendon markers (T1-T7) were detected in the scapular coordinate system using a threshold level of ~1500 Hounsfield units, and 4 virtual humeral bone markers (V1, V2, V3, and V4) were defined at the surface of the lateral edge of the greater tuberosity in the humeral coordinate system (Fig. 1).

Spatial registration of the CT volume to a particular bone model was performed using a modified maximization of mutual information algorithm.[17,34] Each postoperative CT volume was first spatially registered to the humerus bone model of CT_{DOS}, and the coordinates of the humeral bony landmarks and virtual humeral markers were transferred to each postoperative CT volume using the transformation matrix at each time point. Second, each postoperative CT volume was spatially reregistered to the scapula bone model of CT_{DOS}. The previously defined coordinates of the humeral bony landmarks and virtual humeral markers for each scan were transferred into the scapular coordinate system, and the humeral coordinate system was recalculated. These steps resulted in the humeral coordinate system and virtual humeral markers at each postoperative time point being expressed in the scapular coordinate system defined on the CT_{DOS}.

Variation in glenohumeral position

Glenohumeral position was measured in terms of glenohumeral orientation and glenohumeral distance. Glenohumeral orientation was expressed in terms of abduction/adduction, flexion/extension, and internal/external rotation of the humerus relative to the scapula. To accomplish this, we projected the 3D orientation of the humerus onto each plane of the scapular coordinate system and calculated the projected 2D angles between each pair of corresponding axes. Glenohumeral distance was defined as the distance from the glenoid center to the humeral head center (the origins of the 2 coordinate systems) in medial/lateral, anterior/posterior, and superior/inferior directions in the scapular coordinate system. An example of variation in glenohumeral position from the longitudinal scans for a given patient is shown in Figure 2.

Measurement variability in bone-to-tendon marker length measurement

Bone-to-tendon marker length was measured between the coordinates of the virtual humeral markers (V1-V4) on each of the 5 serial CT scans and the coordinates of the tendon markers set at their locations on CT_{DOS} (ie, $V1T1_{DOS}$, $V1T2_{DOS}$, $V2T3_{DOS}$, $V2T4_{DOS}$, $V3T5_{DOS}$, $V3T6_{DOS}$, $V4T7_{DOS}$). An example of variation in bone-to-tendon marker lengths resulting from variation in glenohumeral position across the longitudinal scans for a given patient is shown in Figure 2.

Statistical analysis

Variation across the 5 longitudinal CT scans was summarized, for each glenohumeral position measure and each bone-to-tendon marker length, by the within-patient standard deviation (SD) of the repeated measurements, estimated from 1-way analyses of variance with scans grouped by patient, and by 95% confidence
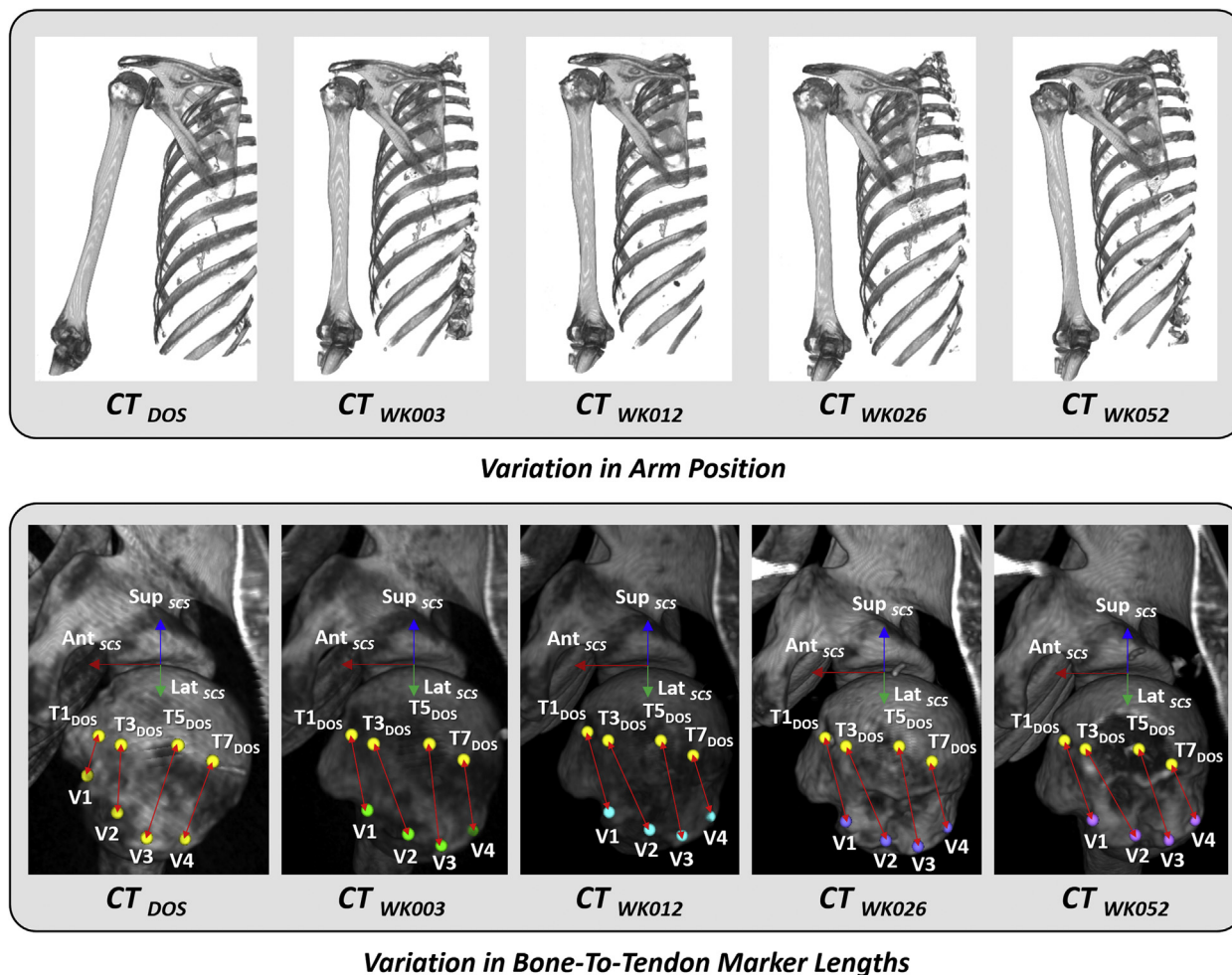
Variation in Arm Position

Variation in Bone-To-Tendon Marker Lengths

Figure 2 (*Top*) Representative longitudinal computed tomographic (CT) images of a given patient throughout the year after rotator cuff repair demonstrate variations in glenohumeral position during scanning. (*Bottom*) The SEMs of bone-to-tendon marker lengths due to the variation in glenohumeral position were estimated by the within-patient SDs of repeated measurements of bone-to-tendon marker lengths between the coordinates of the virtual humeral markers (V1, V2, V3, V4) on each of the 5 longitudinal CT scans and the coordinates of the tendon markers set at their day of surgery (DOS) locations ($T1_{DOS}$, $T3_{DOS}$, $T5_{DOS}$, $T7_{DOS}$). The colors of the virtual humeral markers represent the time of the longitudinal CT images (*yellow*: DOS; *green*: WK003; *turquoise*: WK012; *purple*: WK026; and *pink*: WK052). *WK*, week; *Ant*, anterior; *Lat*, lateral; *Sup*, superior; *SCS*, scapular coordinate system.

intervals (CIs) obtained from the associated underlying chi-square distributions. The within-patient SD for each glenohumeral *position* measure describes its net variability from the combination of pure measurement variability, such as would be seen from replicate scans with glenohumeral position held fixed, and true scan-to-scan changes in glenohumeral position. In contrast, the bone-to-tendon lengths on each scan were measured from the virtual humeral markers to the tendon marker location identified on the CT_{DOS}, after very precise registration of the scapulae[12] and a deterministic translation of the tendon marker location on the CT_{DOS} to the current scan's coordinate system. Hence, variation in these length measurements reflects essentially pure measurement variability, and the within-patient SD in this case is an estimate of the standard error of measurement (SEM) of length. The 95% confidence level minimal detectable distance (MDD) from a fixed point, and minimal detectable change (MDC) between 2 longitudinal length measurements with independent measurement errors, were estimated as $MDD_{95} = 1.96 SEM$ and $MDC_{95} = \sqrt{2} MDD_{95}$, respectively. Parallel boxplots were used to depict measurement spreads for individual patients, and the Brown-Forsythe test to screen for heteroscedasticity (heterogeneous SDs among patients). Statistical computations were performed using the FREQ, UNIVARIATE, and GLM procedures of SAS, version 9.4 (SAS Institute, Inc., Cary, NC, USA).

Results

Patient demographics, tear characteristics, and tendon marker characteristics are summarized in Table I. The average anterior-posterior tear size in this cohort was 2.1 ± 1.0 cm and tears were predominantly isolated to the supraspinatus tendon (32 of 48 patients = 67%). Forty-four of 48 patients (92%) had 2, 3, or 4 implanted tendon markers (range 1-5). The additional operative time to apply the markers at the end of the case was approximately 10-15 minutes. The 48 patients were scanned on 8 different CT scanners (CTDIvol: median 1.78 mGy, IQR 1.75-4.71 mGy; scan length: median 37.7 cm; IQR 35.3-40.0 cm; estimated effective radiation dose per scan: median 0.99 mSv, IQR 0.90-2.28 mSv) by 16 clinical imaging personnel at 6 locations in our health care system.

Variation in glenohumeral position

The mean glenohumeral orientation from the 5 longitudinal CT scans averaged across the 48 patients was 12.6° abduction, 0.4°

Table I
Distributions of patient demographics, tear characteristics, and the number of implanted radiopaque tendon markers in 48 patients undergoing rotator cuff repair surgery

Patient demographics	
Age, yr, mean ± SD	59 ± 8
Sex, n (%)	
Male	25 (52)
Female	23 (48)
BMI, mean ± SD	29.9 ± 6.1
Laterality	
Right	32 (67)
Left	16 (33)
Tear characteristics	
Size, cm, mean ± SD	
AP	2.1 ± 1.0
ML	1.2 ± 0.5
Location, n (%)	
SS	32 (67)
SS+IS	16 (33)
Tendon markers, n (%)	
No. of markers placed	
1	2 (4.2)
2	15 (31.2)
3	19 (39.6)
4	10 (20.8)
5	2 (4.2)

BMI, body mass index; *AP*, antero-posterior; *ML*, medial-lateral; *SS*, supraspinatus only, *SS+IS*, both supraspinatus and infraspinatus.
Mean ± standard deviation for continuous variables, counts and percentages for categorical variables.

flexion, and −0.1° internal rotation (Figs. 3 and 4, Table II). Within a patient, the range of glenohumeral orientation from the 5 CT scans was as small as 5.2° (patient 5) and as large as 25.1° (patient 30) in abduction/adduction, as small as 1.1° (patient 12) and as large as 13.7° (patient 9) in flexion/extension, and as small as 5.2° (patient 39) and as large as 48.2° (patient 16) in internal/external rotation (Fig. 3, Supplementary Appendix S1-S3). For 40 of 48 patients (83%), the highest absolute abduction angle was measured on the CT_{DOS} (Fig. 3, Supplementary Appendix S1). The within-patient SD (95% confidence interval) was least for extension/flexion at 3.0° (2.7°-3.4°) and highest for internal/external rotation at 8.2° (7.3°-9.2°) (Table II). Heteroscedasticity was not statistically significant for any orientation measurement.

Similarly, the mean glenohumeral distance from the 5 longitudinal CT scans averaged across the 48 patients was 25.5 mm lateral, −1.5 mm posterior, and 6.4 mm superior from the glenoid center to humeral head center (Table II). Within a patient, the range of glenohumeral distance from the 5 CT scans was as small as 0.2 mm (patient 40) and as large as 2.5 mm (patient 30) medial/lateral, as small as 0.4 mm (patient 31) and as large as 4.5 mm (patient 44) anterior/posterior, and as small as 0.05 mm (patient 13) and as large as 6.9 mm (patient 30) superior/inferior to the origin of the scapula (Fig. 4). The SDs (95% confidence intervals) of glenohumeral distances were similar in the anterior/posterior (0.9 mm [0.8-1.1 mm]) and superior/inferior (0.9 mm [0.8-1.0 mm]) directions and lower in the medial/lateral direction (0.4 mm [0.3-0.4 mm]) (Table II). Heteroscedasticity was nonsignificant in the anterior/posterior and medial/lateral directions, but there was evidence that measurement variability and hence reliability in the superior/inferior direction itself varies across patients (P = .0003).

Variability in bone-to-tendon marker length measurement

The mean bone-to-tendon marker lengths from the 5 longitudinal CT scans averaged across scans and patients are shown in Table III by marker location across the repair. The respective estimated SEMs ranged from 2.2-2.6 mm for all markers placed, were not statistically distinguishable by marker location, and there was no statistically significant heteroscedasticity. A common estimate for the SEM, pooled across marker locations, was 2.4 mm. Corresponding MDD_{95} values range from 4.3-5.1 mm with a common estimate of 4.7 mm, whereas MDC_{95} values range from 6.1-7.2 mm with a common estimate of 6.7 mm (Table III).

Discussion

To address the need for more objective and quantitative tendon healing measures, we have developed a quantitative method to measure *tendon retraction* following rotator cuff repair using implanted radiopaque markers on the repaired tendon and longitudinal 3D CT imaging.[3,18] We have previously demonstrated the biocompatibility of barium sulfate–infused polypropylene radiopaque tissue markers following 8-12 weeks' implantation in a porcine model, where no radiographic leaching, calcification, or local adverse events were observed.[26] Now, applying and interpreting marker-derived tendon retraction appropriately in the clinical setting requires appreciation of this method's measurement variability. To that end the current study's objectives—recognizing that variation in glenohumeral position during longitudinal scanning likely introduces variability in length measurements[3]—were to assess variation in glenohumeral position among 5 longitudinal CT scans in the first year following rotator cuff repair, and estimate the variabilities in bone-to-tendon marker length measurements due to pragmatic variations in achieving perfect arm repositioning for these scans.

We found that glenohumeral orientation was on average reproducible within approximately 8° of internal/external rotation, 5° of abduction/adduction, and 3° of flexion/extension in a given patient, whereas the center of the humeral head within a patient varied less than 1 mm in any direction in its distance from the center of the glenoid. These findings demonstrate that variation in glenohumeral position on longitudinal CT scanning arises almost exclusively from rotations of the humerus. Several factors may affect reproducibility of glenohumeral position for repeated CT scanning, one being simply the imaging technician's attention to positioning of the arm for scanning in the clinical setting. Sixteen clinical imaging personnel and 8 CT scanners at 6 locations were involved in this study. One day prior to each scan, imaging staff were reminded to "position study patients with their arm at the side," but some variation in glenohumeral position found here is likely explainable simply by inconsistent execution of this instruction. Such variability would likely have been higher without this instruction.

The reproducibility of glenohumeral positioning for longitudinal CT scanning might also be affected by shoulder pain, swelling, body habitus, and/or comfort during lying supine, particularly when such factors change over time. For example, we observed that the highest absolute abduction angle was measured on the CT_{DOS} in 40 of 48 patients (83%) despite removing the sling for scanning (Figs. 3 and 4), possibly explained by immediate postoperative fluid retention in the shoulder. Furthermore, acquiring good-quality images of a shoulder requires positioning the patient off-center on the scanner bed, and the ease of achieving an optimal position varies by the scanner's bore size, patient's girth, and pain at the time. Such patient factors likely contribute to the variation in glenohumeral position reported here.

The variability of bone-to-tendon marker length measurements due to variation in glenohumeral position during longitudinal CT imaging cannot be directly measured because we cannot isolate measurement uncertainty from real structural changes of the tendon over time. Hence, we estimated the variability of bone-to-tendon marker length measurements using the virtual humeral
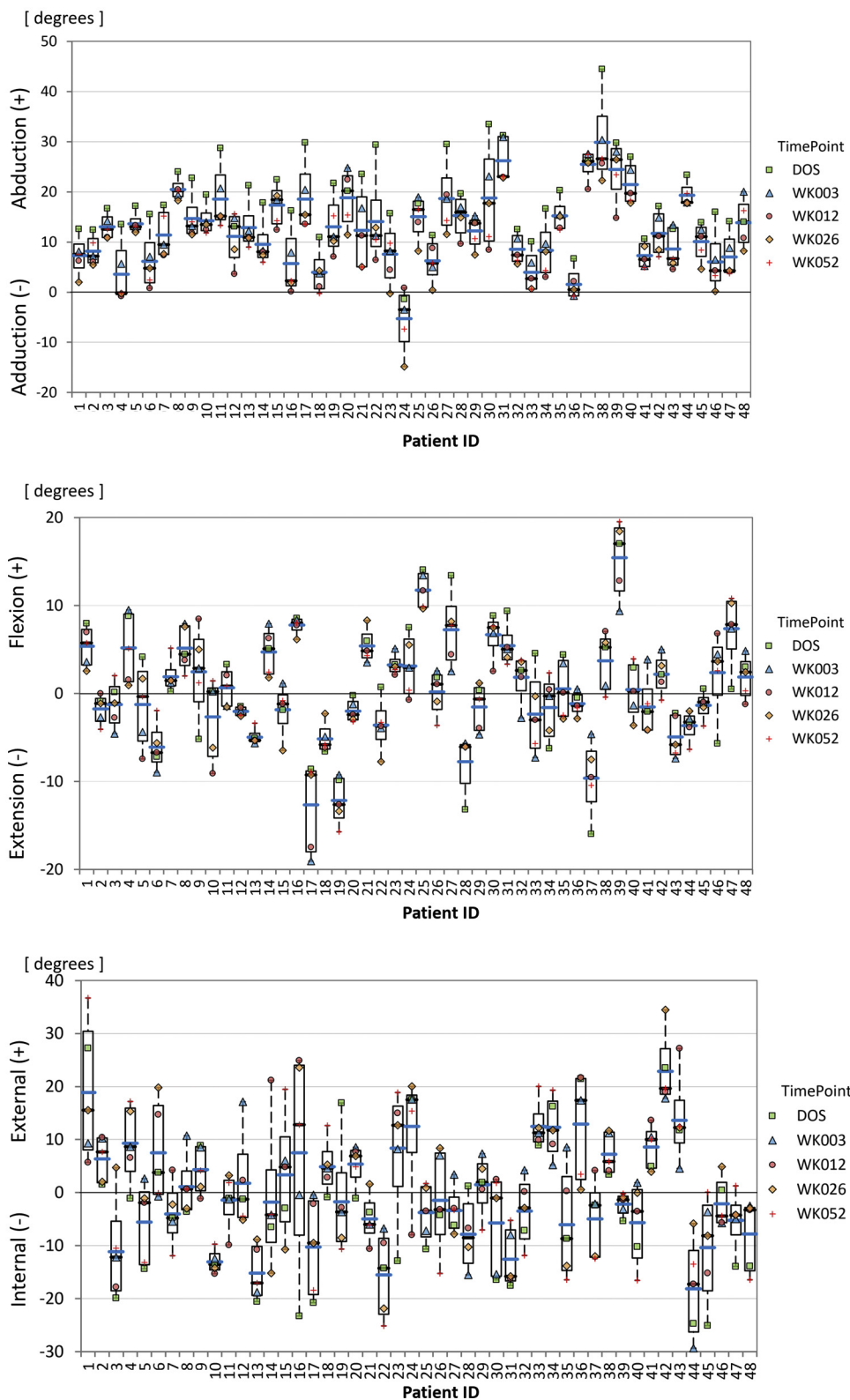
Figure 3 Box and whiskers plot shows minimum, first quartile, median (black line within the box), third quartile, and maximum of repeated measurements of glenohumeral orientation in abduction/adduction (*top panel*), flexion/extension (*middle panel*), and internal/external rotation (*bottom panel*) from 5 longitudinal computed tomographic (CT) scans in each patient. Individual observations within a patient are represented by the time point expressed in the legend. The mean of the repeated measures within a patient is represented with a light-blue line. The mean of the mean glenohumeral orientation from the 5 longitudinal CT scans across the 48 patients was 12.6° abduction, 0.4° flexion, and −0.1° internal rotation. We observed that the highest absolute abduction angle was measured on the day of surgery (DOS) in 40 of 48 patients (83%). *WK*, week.
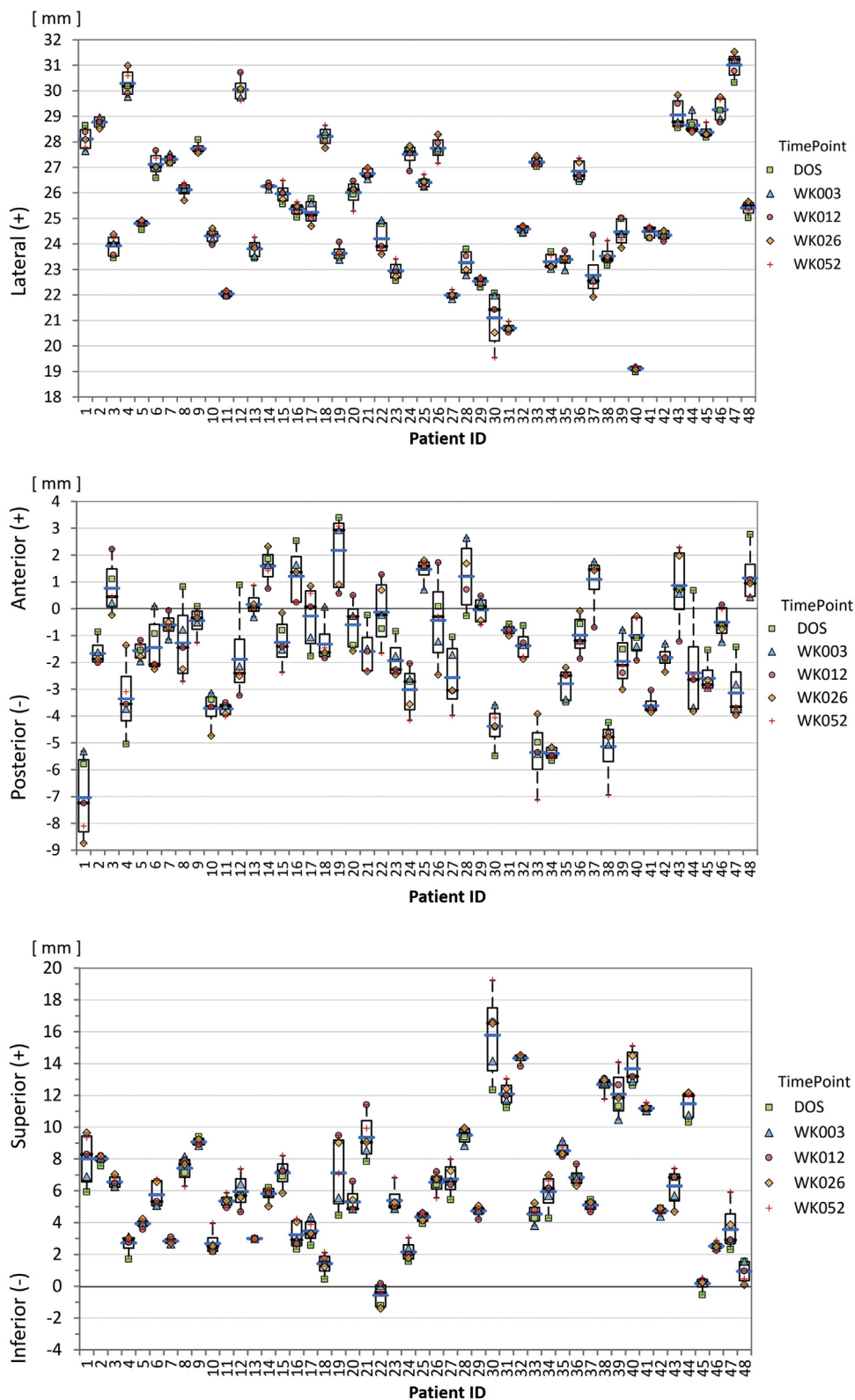
Figure 4 Box and whiskers plot shows minimum, first quartile, median (black line within the box), third quartile, and maximum of repeated measurements of glenohumeral distance in medial/lateral (*top panel*), anterior/posterior (*middle panel*), and superior/inferior (*bottom panel*) from 5 longitudinal computed tomographic (CT) scans in each patient. Individual observations within a patient are represented by the time point expressed in the legend. The mean of the repeated measures within a patient is represented with a light-blue line. The mean of the mean glenohumeral position from the 5 longitudinal CT scans across the 48 patients was 25.5 mm in lateral, −1.5 mm in anterior, and 6.4 mm in superior direction. *WK*, week.

Table II

The mean (range) of glenohumeral orientation and position averaged across the 5 longitudinal CT scans from 48 patients

Glenohumeral position	Mean (range) of patient means from repeated measures	Within-patient SD	95% CI	Heteroscedasticity[*] P value
Glenohumeral orientation, degrees				
Abduction (+) / adduction (−)	12.6 (−5.3 to 29.9)	5.2	4.6-5.8	.99
Flexion (+) / extension (−)	0.4 (−12.7 to 15.4)	3.0	2.7-3.4	.75
External (+) / internal (−) rotation	−0.1 (−18.1 to 22.9)	8.2	7.3-9.2	.75
Glenohumeral distance, mm				
Lateral (+) / medial (−)	25.5 (19.1 to 31.0)	0.4	0.3-0.4	.06
Anterior (+) / posterior (−)	−1.5 (−7.0 to 2.2)	0.9	0.8-1.1	.61
Superior (+) / inferior (−)	6.4 (−0.6 to 15.8)	0.9	0.8-1.0	.0003[†]

CT, computed tomographic; *SD*, standard deviation; *CI*, confidence interval.
Variation in glenohumeral position was assessed by the within-patient SD and 95% CI of orientation and distance measurements.
[*] From Brown-Forsythe test.
[†] Statistically significant heteroscedasticity.

Table III

The mean (range) of bone-to-tendon lengths averaged across the 5 longitudinal CT scans from 48 patients

Bone-to-tendon length Endpoint	n	Mean (range) of means from repeat measures, mm	Estimated SEM, mm	95% CI, mm	Estimated MDD_{95}	Estimated MDC_{95}	Heteroscedasticity[*] P value
$V1T1_{DOS}$	30	20.3 (6.9-29.2)	2.6	2.3-2.9	5.1	7.2	.76
$V1T2_{DOS}$	9	31.8 (25.5-42.5)	2.2	1.9-2.4	4.3	6.1	.51
$V2T3_{DOS}$	44	25.6 (14.8-34.6)	2.5	2.2-2.8	4.9	6.9	.98
$V2T4_{DOS}$	6	33.2 (25.9-38.9)	2.5	2.2-2.8	4.9	6.9	.06
$V3T5_{DOS}$	35	27.6 (15.4-47.0)	2.2	2.0-2.5	4.3	6.1	.96
$V3T6_{DOS}$	2	29.3 (28.2-30.5)	2.3	2.0-2.6	4.5	6.4	.80
$V4T7_{DOS}$	13	27.2 (10.6-47.2)	2.5	2.2-2.8	4.9	6.9	.50

CT, computed tomographic; *SEM*, standard error of measurement; *CI*, confidence interval; MDD_{95}, 95% confidence level minimal detectable distance; MDC_{95}, 95% confidence level minimal detectable change.
The variability in bone-to-tendon length measurements was assessed by the SEM, its 95% CI, and the MDD_{95} and MDC_{95} between 2 distance measurements. Bone-to-tendon length was measured between the coordinates of the virtual humeral markers (V1-V4) on each of the 5 longitudinal CT scans and the coordinates of the tendon markers set at their day of surgery locations on CT_{DOS} ($T1_{DOS}$-$T7_{DOS}$).
[*] From Brown-Forsythe test.

markers on each of the 5 serial CT scans and the coordinates of the tendon markers set at their locations on CT_{DOS}. The resulting SEMs of bone-to-tendon marker lengths associated with variations in glenohumeral position were approximately 2.4 mm (range, 2.2-2.6 mm) and statistically indistinguishable between markers, regardless of the location of the measurement from anterior to posterior across the greater tuberosity. The 2.4-mm value exceeds the analogous SEM of $1.3\text{mm}/\sqrt{2} = 0.9\text{mm}$, derived from the 1.3-mm SD of differences we previously reported from repeated CT imaging in arm positions such as the hand on umbilicus or hand at the side.[3] This is unsurprising, because the prior study's repeated scans were taken in a well-controlled research setting on the same day whereas the current scans were obtained by multiple personnel in different clinical settings and separated by weeks and months, conducive to more variable positioning.

Of the 13 measurement variables studied, only glenohumeral distance in the superior/inferior direction exhibited statistically significant heteroscedasticity. The within-patient SD for this variable target is not a common value for all patients, but rather the quadratic mean (ie, the root mean square) of the distribution of individual within-patient repeated measurement SDs. The highly variable measurements of patients 19 and 30 were the most conspicuous drivers of this result (Fig. 4, bottom panel). Interestingly, patient 30 also had the most variable distribution of medial/lateral and abduction/adduction measurements. Several possible reasons could explain the higher variability in glenohumeral repositioning in these patients as discussed above.

Our findings provide valuable guidance for future research studies using implanted markers to quantify rotator cuff tendon retraction, that is, movement of the repaired tendon away from the humeral head footprint following surgery, which is fundamentally derived from longitudinal measurements of length using 1 of 3 approaches. The first approach is to measure and compute the difference of bone-to-tendon marker lengths on the CT_{DOS} and on any postoperative scan in each CT scan's coordinate system without bony registration.[2,18] The advantage of this approach is that no software or expertise is needed to register the longitudinal CT scans. The disadvantages are the added measurement error associated with needing to localize the positions of the reference markers from the CT_{DOS} on all subsequent scans, and the inability to describe the direction of tendon retraction in an anatomic coordinate system. The second approach measures and computes the difference of bone-to-tendon marker lengths between CT_{DOS} and any later postoperative time, following registration of longitudinal CT volumes to either the scapular or humeral bone models based on the user's interest for a specific anatomic coordinate system. The advantages of volumetric registration, which itself is accurate to 0.1 mm for position and 0.1° for orientation, 13 are the ability to transfer the locations of reference markers from the CT_{DOS} onto longitudinal scans within 0.2mm accuracy (unpublished data), describe the direction of tendon retraction in an anatomic coordinate system, and measure variation in glenohumeral position as well. With either of these first 2 approaches, however, measurement variation must be accounted for in both distance measurements. Based on our data, the minimally detectable retraction measured in this manner would be 6.7 mm (MDC_{95}).

Third, rotator cuff tendon retraction can also be estimated by measuring a single distance between a tendon marker's location on

the CT_{DOS} and its later location at any subsequent time point following scapular registration of longitudinal CT volumes. This approach of measuring tendon marker-to-tendon marker length limits variation to only a single distance measurement from a tendon marker's reference position on the CT_{DOS} to its position at any later time. We believe the minimally detectable distance (MDD_{95}) for measuring a single bone-to-tendon marker length estimated at 4.7 mm in this study is a reasonable estimate for tendon marker-to-tendon marker MDD, and may actually be a conservative estimate because tendon markers affixed to the compliant rotator cuff tendon medial to its bony insertion are probably less likely to be influenced by variations in humeral position than bone markers rigidly attached to the greater tuberosity. As a point of reference, we note that others have arbitrarily assigned 5 mm as the level of uncertainty of rotator cuff tendon tear size measurements made on MRI and ultrasonography.[31]

There are a couple of noteworthy limitations to the work reported here. First, although this study estimated uncertainty introduced in length measures from variable positioning of the glenohumeral joint, it does not address measurement uncertainty from imprecision in tendon marker localization over time. In particular, tendon markers that derive from radiopaque suture knots may orient variably on longitudinal scans, leading to variation in the location of their centroids. Because the knot stacks comprising the markers are approximately 4 mm tall, we estimate any added variability from localization of their centroid to be within ± 2 mm. Furthermore, based on our observations using these markers in animal models,[26] fibrous tissue likely forms around the suture knots such that their orientation is not continuously changing beyond the early postoperative period, so it is very possible that this source of variation becomes negligible after 3-4 weeks. It should also be noted that this study did not assess the validity of tendon retraction measurements. Errors could arise from tendon markers moving, slipping or breaking away from the location where placed, and validity will be assessed in future work.

In summary, the aim of this article was to measure the variability in glenohumeral positioning among longitudinal CT scans and estimate associated measurement variability introduced in marker-based measurements of tendon retraction. Repeating a standard shoulder CT imaging protocol 5 times over 1 year postoperatively in the clinical setting resulted in within-patient SDs of glenohumeral orientation of 8° of internal/external rotation, 5° of abduction/adduction, and 3° of flexion/extension. The associated estimated SEM of bone-to-tendon length was 2.4 mm with an MDD_{95} of 4.7 mm, which we believe are also reasonable estimates for the SEM and MDD_{95} of tendon marker-to-tendon marker lengths that can be used as estimates of tendon retraction. Therefore, apparent changes in tendon retraction of 5 mm or more, when measured as the distance from a tendon marker's location at CT_{DOS} to its new location on a volumetrically registered longitudinal CT scan, may be considered above the usual range of measurement variation.

Conclusion

Tendon retraction measured from implanted radiopaque tendon markers and longitudinal low-dose CT scanning offers a sufficiently reliable means for objectively measuring the commonly expected changes in structural healing following rotator cuff repair, though its potential clinical significance must be demonstrated and is the aim of our ongoing work (https://clinicaltrials.gov/ct2/show/NCT02716441). We anticipate that incorporating the magnitude, timing, location, and direction of tendon retraction as well as the continuity of the repaired tissue from traditional imaging will yield an improved understanding of rotator cuff tendon healing, allowing for advances in treatment strategies that improve surgical healing and clinical outcomes and result in more durable rotator cuff repairs over time. At the current time, we anticipate that tendon retraction measured from implanted radiopaque tendon markers and longitudinal low-dose CT scanning will find its primary utility as a research tool. However, if its significance as a clinically meaningful measure of structural healing following rotator cuff repair is demonstrated by our ongoing research, future work to understand the mechanisms of tendon retraction and to develop broadly applicable clinical methods for measuring tendon retraction following rotator cuff repair would be justified.

Supplementary Data

Supplementary data to this article can be found online at https://doi.org/10.1016/j.jseint.2020.08.001.

References

1. Barber FA, Hrnack SA, Snyder SJ, Hapa O. Rotator cuff repair healing influenced by platelet-rich plasma construct augmentation. Arthroscopy 2011;27: 1029−35. https://doi.org/10.1016/j.arthro.2011.06.010.
2. Baring TK, Cashman PP, Reilly P, Emery RJ, Amis AA. Rotator cuff repair failure in vivo: a radiostereometric measurement study. J Shoulder Elbow Surg 2011;20:1194−9. https://doi.org/10.1016/j.jse.2011.04.010.
3. Derwin KA, Milks RA, Davidson I, Iannotti JP, McCarron JA, Bey MJ. Low-dose CT imaging of radio-opaque markers for assessing human rotator cuff repair: accuracy, repeatability and the effect of arm position. J Biomech 2012;45:614−8. https://doi.org/10.1016/j.jbiomech.2011.11.046.

4. Fuchs B, Gilbart MK, Hodler J, Gerber C. Clinical and structural results of open repair of an isolated one-tendon tear of the rotator cuff. J Bone Joint Surg Am 2006;88:309–16. https://doi.org/10.2106/JBJS.E.00117.

5. Galatz LM, Ball CM, Teefey SA, Middleton WD, Yamaguchi K. The outcome and repair integrity of completely arthroscopically repaired large and massive rotator cuff tears. J Bone Joint Surg Am 2004;86:219–24.

6. Gladstone JN, Bishop JY, Lo IK, Flatow EL. Fatty infiltration and atrophy of the rotator cuff do not improve after rotator cuff repair and correlate with poor functional outcome. Am J Sports Med 2007;35:719–28. https://doi.org/10.1177/0363546506297539.

7. Goutallier D, Postel JM, Bernageau J, Lavau L, Voisin MC. Fatty muscle degeneration in cuff ruptures. Pre- and postoperative evaluation by CT scan. Clin Orthop Relat Res 1994;304:78–83.

8. Haque A, Pal Singh H. Does structural integrity following rotator cuff repair affect functional outcomes and pain scores? A meta-analysis. Shoulder Elbow 2018;10:163–9. https://doi.org/10.1177/1758573217731548.

9. Hasegawa A, Mihata T, Yasui K, Kawakami T, Itami Y, Neo M. Intra- and inter-rater agreement on magnetic resonance imaging evaluation of rotator cuff integrity after repair. Arthroscopy 2016;32:2451–8. https://doi.org/10.1016/j.arthro.2016.04.027.

10. Iannotti JP, Codsi MJ, Kwon YW, Derwin K, Ciccone J, Brems JJ. Porcine small intestine submucosa augmentation of surgical repair of chronic two-tendon rotator cuff tears. A randomized, controlled trial. J Bone Joint Surg Am 2006;88:1238–44. https://doi.org/10.2106/JBJS.E.00524.

11. Iannotti JP, Deutsch A, Green A, Rudicel S, Christensen J, Marraffino S, et al. Time to failure after rotator cuff repair: a prospective imaging study. J Bone Joint Surg Am 2013;95:965–71. https://doi.org/10.2106/JBJS.L.00708.

12. Iannotti JP, Ricchetti ET, Rodriguez EJ, Bryan JA. Development and validation of a new method of 3-dimensional assessment of glenoid and humeral component position after total shoulder arthroplasty. J Shoulder Elbow Surg 2013;22:1413–22. https://doi.org/10.1016/j.jse.2013.01.005.

13. de Jesus JO, Parker L, Frangos AJ, Nazarian LN. Accuracy of MRI, MR arthrography, and ultrasound in the diagnosis of rotator cuff tears: a meta-analysis. AJR Am J Roentgenol 2009;192:1701–7. https://doi.org/10.2214/ajr.08.1241.

14. Kluger R, Bock P, Mittlbock M, Krampla W, Engel A. Long-term survivorship of rotator cuff repairs using ultrasound and magnetic resonance imaging analysis. Am J Sports Med 2011;39:2071–81. https://doi.org/10.1177/0363546511406395.

15. Koh KH, Kang KC, Lim TK, Shon MS, Yoo JC. Prospective randomized clinical trial of single- versus double-row suture anchor repair in 2- to 4-cm rotator cuff tears: clinical and magnetic resonance imaging results. Arthroscopy 2011;27:453–62. https://doi.org/10.1016/j.arthro.2010.11.059.

16. Liem D, Lichtenberg S, Magosch P, Habermeyer P. Magnetic resonance imaging of arthroscopic supraspinatus tendon repair. J Bone Joint Surg Am 2007;89:1770–6. https://doi.org/10.2106/JBJS.F.00749.

17. Maes F, Collignon A, Vandermeulen D, Marchal G, Suetens P. Multimodality image registration by maximization of mutual information. IEEE Trans Med Imaging 1997;16:187–98.

18. McCarron JA, Derwin KA, Bey MJ, Polster JM, Schils JP, Ricchetti ET, et al. Failure with continuity in rotator cuff repair "healing". Am J Sports Med 2013;41:134–41. https://doi.org/10.1177/0363546512459477.

19. Niglis L, Collin P, Dosch JC, Meyer N, Kempf JF. Intra- and inter-observer agreement in MRI assessment of rotator cuff healing using the Sugaya classification 10 years after surgery. Orthop Traumatol Surg Res 2017;103:835–9. https://doi.org/10.1016/j.otsr.2017.06.006.

20. Park JS, Park HJ, Kim SH, Oh JH. Prognostic factors affecting rotator cuff healing after arthroscopic repair in small to medium-sized tears. Am J Sports Med 2015;43:2386–92. https://doi.org/10.1177/0363546515594449.

21. Park JY, Lhee SH, Oh KS, Moon SG, Hwang JT. Clinical and ultrasonographic outcomes of arthroscopic suture bridge repair for massive rotator cuff tear. Arthroscopy 2013;29:280–9. https://doi.org/10.1016/j.arthro.2012.09.008.

22. Raman J, Walton D, MacDermid JC, Athwal GS. Predictors of outcomes after rotator cuff repair—a meta-analysis. J Hand Ther 2017;30:276–92. https://doi.org/10.1016/j.jht.2016.11.002.

23. Rodeo SA, Delos D, Williams RJ, Adler RS, Pearle A, Warren RF. The effect of platelet-rich fibrin matrix on rotator cuff tendon healing: a prospective, randomized clinical study. Am J Sports Med 2012;40:1234–41. https://doi.org/10.1177/0363546512442924.

24. Russell RD, Knight JR, Mulligan E, Khazzam MS. Structural integrity after rotator cuff repair does not correlate with patient function and pain: a meta-analysis. J Bone Joint Surg Am 2014;96:265–71. https://doi.org/10.2106/JBJS.M.00265.

25. Saccomanno MF, Sircana G, Cazzato G, Donati F, Randelli P, Milano G. Prognostic factors influencing the outcome of rotator cuff repair: a systematic review. Knee Surg Sports Traumatol Arthrosc 2016;24:3809–19. https://doi.org/10.1007/s00167-015-3700-y.

26. Sahoo S, Baker AR, Jun BJ, Erdemir A, Ricchetti ET, Iannotti JP, et al. A novel radiopaque tissue marker for soft tissue localization and in vivo length and area measurements. PloS One 2019;14:e0224244. https://doi.org/10.1371/journal.pone.0224244.

27. Slabaugh MA, Nho SJ, Grumet RC, Wilson JB, Seroyer ST, Frank RM, et al. Does the literature confirm superior clinical results in radiographically healed rotator cuffs after rotator cuff repair? Arthroscopy 2010;26:393–403. https://doi.org/10.1016/j.arthro.2009.07.023.

28. Sugaya H, Maeda K, Matsuki K, Moriishi J. Functional and structural outcome after arthroscopic full-thickness rotator cuff repair: single-row versus dual-row fixation. Arthroscopy 2005;21:1307–16. https://doi.org/10.1016/j.arthro.2005.08.011.

29. Sugaya H, Maeda K, Matsuki K, Moriishi J. Repair integrity and functional outcome after arthroscopic double-row rotator cuff repair. A prospective outcome study. J Bone Joint Surg Am 2007;89:953–60. https://doi.org/10.2106/JBJS.F.00512.

30. Tashjian RZ, Hollins AM, Kim HM, Teefey SA, Middleton WD, Steger-May K, et al. Factors affecting healing rates after arthroscopic double-row rotator cuff repair. Am J Sports Med 2010;38:2435–42. https://doi.org/10.1177/0363546510382835.

31. Teefey SA, Rubin DA, Middleton WD, Hildebolt CF, Leibold RA, Yamaguchi K. Detection and quantification of rotator cuff tears. Comparison of ultrasonographic, magnetic resonance imaging, and arthroscopic findings in seventy-one consecutive cases. J Bone Joint Surg Am 2004;86:708–16.

32. Thomazeau H, Boukobza E, Morcet N, Chaperon J, Langlais F. Prediction of rotator cuff repair results by magnetic resonance imaging. Clin Orthop Relat Res 1997:275–83.

33. Toussaint B, Schnaser E, Bosley J, Lefebvre Y, Gobezie R. Early structural and functional outcomes for arthroscopic double-row transosseous-equivalent rotator cuff repair. Am J Sports Med 2011;39:1217–25. https://doi.org/10.1177/0363546510397725.

34. Wells WM 3rd, Viola P, Atsumi H, Nakajima S, Kikinis R. Multi-modal volume registration by maximization of mutual information. Med Image Anal 1996;1:35–51.

35. Wu G, van der Helm FCT, Veeger HEJ, Makhsous M, Van Roy P, Anglin C, et al. ISB recommendation on definitions of joint coordinate systems of various joints for the reporting of human joint motion, part II: shoulder, elbow, wrist and hand. J Biomech 2005;38:981–92. https://doi.org/10.1016/j.jbiomech.2004.05.042.